JOURNAL OF APPLIED ELECTROCHEMISTRY 26 (1996) 959–967

Chemical and morphological characterization of a direct methanol fuel cell based on a quaternary Pt–Ru–Sn–W/C anode

A. S. ARICÒ, P. CRETÌ, N. GIORDANO, V. ANTONUCCI

Institute CNR–TAE, via Salita S. Lucia sopra Contesse 39, 98126 S. Lucia Messina, Italy

P. L. ANTONUCCI

Institute of Chemistry, Faculty of Engineering, University of Reggio Calabria, via E. Cuzzocrea 48, 89100 Reggio Calabria, Italy

A. CHUVILIN

Institute of Catalysis, 630090 Novosibirsk, Russia

Received 30 October 1995; revised 13 January 1996

Conventional and 'paste process' methods were investigated to fabricate the membrane/electrode assembly (M&E) for application in a vapour-feed direct methanol fuel cell. A quaternary Pt–Ru–Sn–W/C and a Pt/C catalysts were employed for methanol oxidation and oxygen reduction, respectively. The structure and chemical composition of the catalysts were investigated by transmission electron microscopy (TEM) and X-ray powder diffraction (XRD). A crystalline Pt f.c.c. phase was found to prevail in both catalysts. Agglomeration and twinned particles were frequently observed in the Pt–Ru–Sn–W/C catalyst. Electrochemical investigations were performed by a.c.-impedance spectroscopy and galvanostatic polarization. The 'paste process' based assembly showed a significantly lower uncompensated resistance and an approximately two-fold power density increase with respect to the conventional assembly. According to the scanning electron microscopy analysis the observed results were attributed to improved bonding between catalysts and perfluorosulfonic membrane and to a larger extension of the three-phase reaction zone in the 'paste process' based assembly.

1. Introduction

In recent years an increasing interest has been directed towards the development of direct methanol fuel cells (DMFCs) based on a proton-exchange membrane electrolyte [1–3]. Interesting results have recently been obtained with vapour-feed DMFCs [2, 3]. These fuel cells operate at temperatures between 100 °C and 130 °C and include a Pt–Ru (1 : 1, at.) anode, a Pt cathode and a Nafion® 117 membrane [2, 3]. A high loading of noble metals, that is, 4–5 mg Pt cm^{-2} [2, 3] at both electrodes is used as a consequence of the poor electrocatalytic activity of the anode and partial cathode poisoning due to the methanol cross-over through the membrane. DMFCs based on this loading are a long way from practical applicability. A much lower Pt loading is employed in the liquid-feed DMFC [1], that is, 0.5 mg Pt cm^{-2}, yet, this cell has shown a lower fuel utilization with respect to the vapour-feed fuel cell [2].

Recent advances in the realization of the membrane-electrode (M&E) assembly for solid polymer electrolyte fuel cells (SPEFCs) have concerned the removal of polytetrafluoroethylene (Teflon) binder from the catalytic layer in the electrodes [4–6]. According to Wilson and Gottesfeld [4], the ionic path in the catalytic layer due to the recast ionomer is hindered on the catalyst surface and pores covered and/or blocked by Teflon particles. These considerations may be extended to DMFCs and, hence, new electrode and M&E assembly preparation methods should be investigated. Among the various methods, the 'paste process' developed by Uchida *et al.* [6] seems to be more suitable for the DMFC. In fact, it would not, in principle, favour methanol cross-over and, moreover, it does not require a laborious procedure.

A previous paper [7], describes a preliminary investigation of the electroactivity of a quaternary Pt–Ru–Sn–W/C catalyst for methanol oxidation in halfcell. The formulation of a quaternary catalyst containing transition metal oxides, has been suggested by its suitable characteristics in terms of redox functionalities in the potential range of methanol oxidation. Spectroscopic and crystallographic analyses have shown that the oxide functionalities act through their electron accepting and donating sites, and therefore

0021-891X

promote the oxidation of methanol and CO-related species [7]. Moreover, transition metal oxides, because of their partially filled orbitals, may allow a labile interaction with carbon monoxide and also have the ability to chemisorb hydroxyl species on neighbouring sites. Accordingly, the quaternary catalyst demonstrated higher activity with respect to bimetallic systems obtained in similar way [7].

The present paper compares the operational characteristics of two M&E assemblies based on conventional [8] and 'paste process' [6] methods in a vapour-feed DMFC. The quaternary Pt–Ru–Sn–W/C catalyst included in the M&E assembly has been investigated by TEM and XRD.

2. Experimental details

2.1. *Preparation and characterization of catalysts*

The carbon supported Pt–Ru–Sn–W/C catalyst for methanol oxidation was obtained by liquid-phase reduction of chloroplatinic acid, tin chloride, ruthenium chloride and ammonium metatungstate precursors with hydrazine in an acidic solution. Vulcan XC 72-R carbon black was thermally treated in a quartz tube furnace under flowing nitrogen atmosphere at 900 °C for 2 h before being suspended in water at 70 °C under ultrasonic stirring. Appropriate amounts of H_2PtCl_6, $(NH_4)_6H_2W_{12}O_{40}$, $SnCl_2$ and $RuCl_3$ in a hydrochloric acid solution (Pt : Ru : Sn : W molar ratio equal to 3 : 1 : 1 : 1) were added to the carbon suspension in order to obtain about 60% total metal loading on carbon black. Reduction was performed by dropwise addition of an excess amount of 0.2 M N_2H_4 solution. The reduction process was monitored by recording the redox potential variation of the suspension [7]. The N_2H_4 addition was stopped when no significant variation of the redox potential was recorded in a suitable range. Subsequently, the catalyst was filtered and well washed; the filtrate solution was analysed by a Hitachi u.v.–vis. spectrophotometer in the range 800–200 nm to detect losses of soluble precursors. The obtained catalyst was dried in an air oven at 110 °C for 4 h. The composition of the metallic compounds in the quaternary catalyst was Pt 36.6%, Ru 6.2%, Sn 7.2% and W 11.2%, by weight. A 20% Pt/Vulcan XC 72R catalyst for oxygen reduction was purchased from ElectroChem. Inc. (Woburn, MA).

XRD analysis of the catalysts for methanol oxidation and oxygen reduction was carried out with a Philips X-Pert PW 3710 X-ray powder diffractometer using CuK_α radiation source. Transmission electron microscopy analysis was performed using a TEM apparatus (Philips CM 12) whose ultimate spatial resolution was 200 pm. Catalysts were ground to obtain a very fine powder and dispersed in isopropyl alcohol using ultrasonic treatment. A drop of this dispersion was deposited and dried on a standard Cu grid covered with carbon film.

2.2. *Preparation and characterization of the membrane/electrode assembly*

Two preparation procedures were investigated for the operation of the M&E assembly in DMFC. The backing layers were similar in the two procedures and were prepared as follows: the activated carbon black (Vulcan XC-72) was mixed with water at 60 °C in an ultrasonic bath with mechanical stirring for about 30 min. Subsequently, the slurry was further agitated for 30 min. An appropriate amount of isopropyl alcohol was added and the slurry left to wet for 2 h. The flocculate was spread by a doctor-blade technique over a Stackpole carbon cloth (Stackpole Fibers Company, Lowell, MA, USA) wet-proofed with PTFE solution. The backing layers were pressed at 70 °C for 1 h under 3 MPa compacting load and then sintered at 350 °C for 35 min in air. The total loading of carbon black and PTFE in the diffusion layer after thermal sintering was 3 mg cm^{-2}.

2.2.1. Method A. The first method (A) is based on a conventional procedure developed by Srinivasan *et al.* [8]. Gas-diffusion electrodes were prepared by depositing the Teflon bonded Pt–Ru–Sn–W/C (anode) and Pt/C (cathode) catalysts on carbon cloth backings acting as diffusion layers. The catalyst layer ink was prepared in the same way as in the diffusion layer procedure and deposited on the already prepared backings. Appropriate amounts of catalyst and PTFE suspension were deposited in order to have 1 mg Pt cm^{-2} and 0.5 mg Pt cm^{-2} contents at anode and cathode, respectively, and 30% PTFE loading in both catalytic layers. A 5% Nafion® solution (Nafion® 117, Solution Technology, Inc.) was spread onto the electrode surface to form a film (1 mg Nafion® per cm^2) after solvent evaporation by drying in vacuum for 1 h at 70 °C. The Pt–Ru–Sn–W/C anode and the Pt/C cathode both coated with Nafion® film were hot-pressed on both sides of a purified Nafion® 117 membrane (Du Pont de Nemours) at 100 °C and 1 atm for 5 min and thereafter at 130 °C and 50 atm for 90 s followed by rapid cooling at room temperature.

2.2.2. Method B. In this method the catalytic layer in the electrodes does not contain Teflon binder. Furthermore, a colloid perfluorosulfonated ionomer (PFSI) is applied to the catalyst, thus acting both as ionic electrolyte and as binder between the catalyst particles [6]. Accordingly, a 5% Nafion® solution was mixed in a beaker with butyl acetate to obtain a colloidal suspension. The catalyst powder was then added to this suspension and stirred in an ultrasonic bath. The ultrasonic treatment was stopped when the slurry had been transformed into a paste. A weight ratio of 1 : 2 : 25, Nafion® (dry weight) : catalyst : butyl acetate, was adopted for both anode and cathode. The paste based on the Pt–Ru–Sn–W/C catalyst was spread by a doctor blade technique over the backing layer to form the anode while the paste

of Pt/C catalyst was spread on a Teflon film to form the cathode according to the procedure described by Wilson and Gottesfeld [4]. Pt loadings in this M&E assembly were 1 mg cm^{-2} at the anode and 0.35 mg cm^{-2} at the cathode. Both electrodes were hot-pressed to a Nafion® 117 membrane at 150 °C and 90 atm for 1 min. The Teflon film was removed from the cathode side in the M&E assembly and the previously prepared backing was applied to the cathode during installation of the M&E assembly into the fuel cell housing.

2.3. *Single cell*

The electrode-membrane assemblies, having geometrical electrode area of 50 cm^2 were loaded into a single cell test fixture composed of two copper current collector end plates and two graphite plates containing rib-channel patterns allowing the passage of methanol vapour at the anode and humidified oxygen at the cathode. A 2 M CH_3OH solution was supplied to a vaporizer maintained at 130 °C and fed at atmospheric pressure into the cell at the rear of the anode. The water in the oxygen humidifier was maintained during cell startup and M&E assembly testing at a temperature of 5 °C higher than the cell temperature. Humidified oxygen was fed to the cathode at 3 atm.

Methanol cross-over was investigated by the following procedure. The cathode outlet, composed of exhaust oxygen and water vapour, was connected to a water bubbler before being vented to the atmosphere. The water vapour in the oxygen stream, accompanies the methanol vapour which reaches the cathode. This was condensed in the water bubbler forming a diluted methanol solution that was analysed by gas-chromatography.

The cell was connected to a HP 6060B electronic load and steady-state galvanostatic measurements were performed to investigate the electrochemical activity. Uncompensated resistance (R_u) was measured by both the current interruption method using a Philips memory oscilloscope, during cell operation, and a.c.-impedance spectroscopy using a Solartron 1260 instrument under open circuit conditions.

Several M&E assemblies were investigated for each preparation procedure. The results were found to be reproducible within ±5% around the average value for the electrical power density. The steady-state open circuit voltages changed by less than 30 mV for the various samples within each preparation method.

The morphology and composition of the M&E assembly was investigated using a Philips XL20 scanning electron microscope operating at an accelerating voltage of 20 kV and equipped with an energy dispersive X-ray analysis (EDAX) microprobe. Concentrations of the various elements were derived by the ZAF intensity correction algorithm. Micrographs and chemical profile measurements were taken on cross-sections of the electrochemically tested M&E assemblies.

3. Results and discussion

3.1. *X-ray diffraction analysis*

Figure 1 shows the X-ray diffraction patterns of 60% Pt–Ru–Sn–W/C and 20% Pt/C catalysts. Both catalyst samples exhibit the characteristic diffraction peaks of the Pt f.c.c. structure (JCPDS 4-802). The Pt diffraction peaks in the Pt–Ru–Sn–W/C catalyst are shifted at higher values of 2θ with respect to the Pt/C sample. This corresponds to a decrease in the lattice parameter from 392.1 pm in Pt/C to 390.6 pm in the multifunctional catalyst, probably due to the formation of a Pt–Ru [9] and/or Pt_2W (JCPDS 431361) alloys. No evidence of peaks related to Pt_3Sn (JCPDS 35-1360) and PtSn (JCPDS 8-192) alloys was found. Small diffraction peaks (Fig. 1) were related to the presence of a SnO_2 phase (JCPDS 411445). The first peak at 26.13° in the XRD pattern

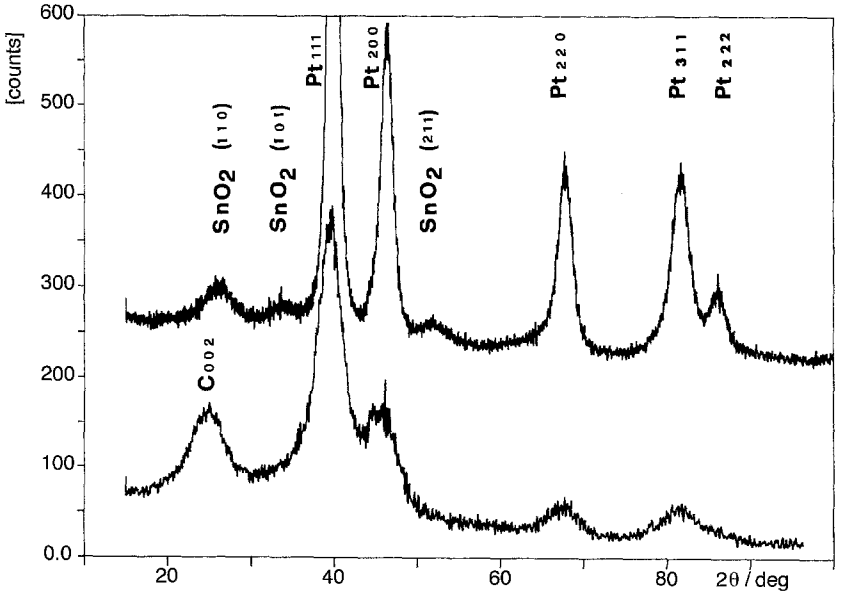

Fig. 1. X-ray diffraction pattern of carbon supported catalysts. C indicates the graphitic carbon (0 0 2) reflection peak.

of Pt–Ru–Sn–W/C catalyst is a convolution of the (0 0 2) reflection of the graphitic carbon layers and the (1 1 0) reflection of SnO_2 (JCPDS 411445). XPS analyses of a Pt–Ru–Sn–W/C catalyst [7] have clearly shown the presence of RuO_2, SnO_2 as well as WO_2 and WO_3 species. The average Pt particle size in the two catalysts was determined from the broadening of the (2 2 0) reflection of the Pt f.c.c. lattice (Fig. 1) by using the Debye–Sherrer equation. The measured full width at half maximum (FWHM) value was corrected for instrumental broadening by using the Warren formula [10]. The average Pt particle size was 2.3 nm for the 20% Pt/C catalyst and 4.8 nm for the 60% Pt–Ru–Sn–W/C catalyst. The estimated error based on the peak profile fitting is ±5%.

3.2. *Transmission electron microscopy analysis*

The dispersion of metal particles on the carbon support for both 20% Pt/Vulcan (cathode) and 60% Pt–Ru–Sn–W (3 : 1 : 1 : 1)/Vulcan anode was investigated by TEM. The 20% Pt/C catalyst showed a homogeneous Pt dispersion (Fig. 2) with particle size ranging between 1.5 and 4.0 nm. The average particle size was 2.5 nm in close agreement with the value determined by XRD.

Electron micrographs of the 60% Pt–Ru–Sn–W/C catalyst (Figs 3 and 4) showed that metal particles are mainly formed by agglomeration of several crystallites. The dispersion of metal clusters in the multicomponent catalyst is less homogeneous than in the case of the Pt/C catalyst; furthermore, an elongated shape

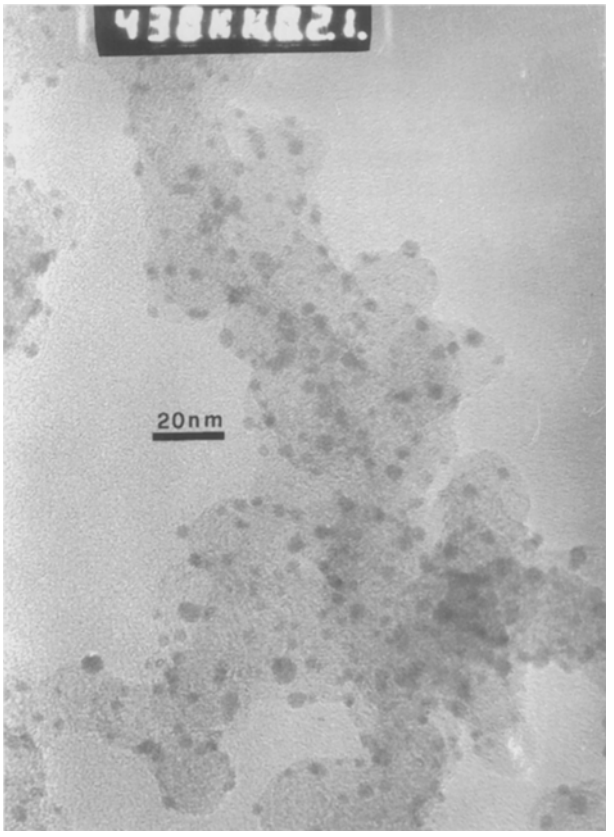

Fig. 2. Bright field TEM micrograph of Pt/C catalyst.

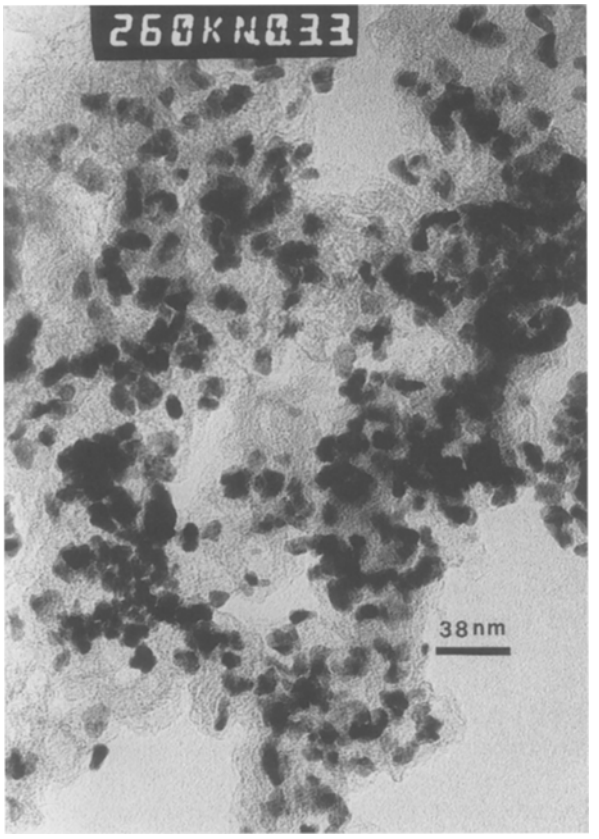

Fig. 3. Bright field TEM micrograph of Pt–Ru–Sn–W/C catalyst.

is frequently observed for the metal particles in the Pt–Ru–Sn–W/C catalyst as opposite to the spherical shape of Pt/C crystallites. The size of the primary particles and the agglomerates in the multicomponent catalyst ranged between 3.0 and 10.0 nm. No precise

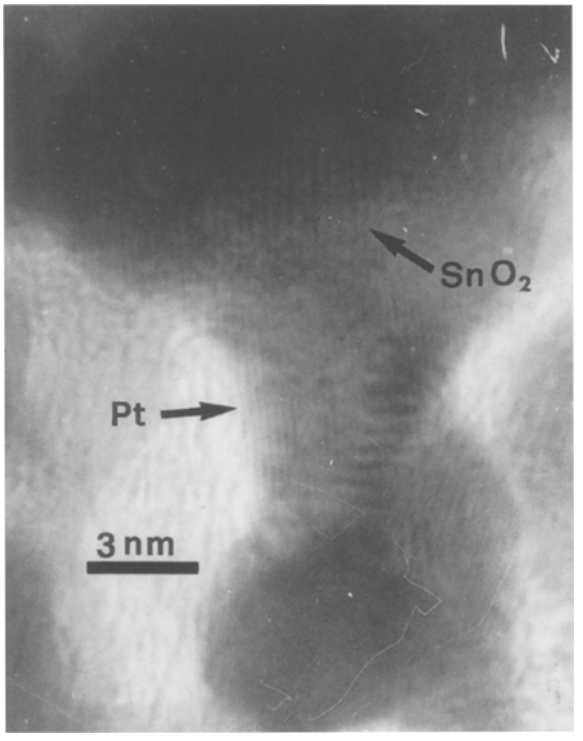

Fig. 4. Bright field image of a Pt–Ru–Sn–W/C catalyst region characterized by moiré and twinned particles.

estimation of the average particle size was possible in this case.

The absence of an appropriate internal standard in our samples made the precise measurements of the observed interlayer distances impossible (Fig. 4). Therefore, we could not ascertain from TEM the presence of alloyed Pt particles. XRD analysis of the multicomponent catalyst indicates the presence of Pt in the form of metal crystallites with a mean particle size of 4.8 nm and Sn, Ru and W in the form of nanocrystalline or amorphous structure. Yet, the estimated change in the Pt lattice parameter suggests a partial alloying of Pt with Ru and/or W.

Moiré and twinned particles (Fig. 4) were observed in the Pt–Ru–Sn–W/C catalyst. These features and the irregular particle shape, are characteristic of the multicomponent catalyst as they were not detected in the Pt/C catalyst with similar metal loading and prepared in similar conditions. To gain deeper information, micrographs such as that of Fig. 4 were computer-acquired and on the corresponding Fourier filtered image, diffraction patterns corresponding to selected lattice regions were obtained. From this analysis it was possible to ascertain that the twinned particle region is characterized by the same lattice parameters. As discussed above, the absence of an internal calibration precludes the precise determination of the interlayer distance. Yet, a rough estimation is possible by using the d (0 0 2) interlayer spacing of graphitic carbon support. Calibration was made with several aligned carbon layers in regions where carbon lattice appeared sufficiently regular. The interlayer spacing in the twinned particle region in Fig. 4 is thus attributed to (1 1 1) planes of the Pt f.c.c. lattice. A significantly larger interlayer spacing is observed in the upper side of Fig. 4. This latter is attributed to the (1 1 0) interlayer distance of the SnO_2 cassiterite. Although a possible interference from carbon support could be taken into account, the high level of ordering observed in this region is not typical of the carbon black substrate. These observations suggest that an overlapping between the different lattices of Pt and metal oxide particles may occur in this catalyst.

3.3. *Electrochemical testing*

After inserting a new M&E assembly into the single cell test housing, the anode and the cathode backing layers were fed with distilled water and pressurized humidified oxygen (3 atm), respectively, at a temperature 5 °C higher than the cell temperature. The cell was warmed-up to 90 °C stepwise and a.c.-impedance spectra were collected at various temperatures. The series resistance (R_s) of the DMFC cell was determined from the high frequency intercept on the real axis of the Nyquist plot. R_s decreased rapidly as temperature increased, as the main contribution to the series resistance is due to the ionic resistance of the membrane and recast ionomer in the catalytic layer. Figure 5 shows a comparison of the variation of the series resistance as a function of temperature for the two assemblies. The M&E assembly prepared according to method B shows significantly lower series resistance with respect to that prepared according to method A, although, the two assemblies are based on the same membrane i.e. Nafion® 117 with the same amount of loaded ionomer. Various M&E assemblies were fabricated and the impedance results were found to be highly reproducible.

A 2 M methanol solution was fed to the anode through a vaporizer maintained at 130 °C, while the cell temperature was raised to 95 °C and various galvanostatic polarizations were carried out. It was

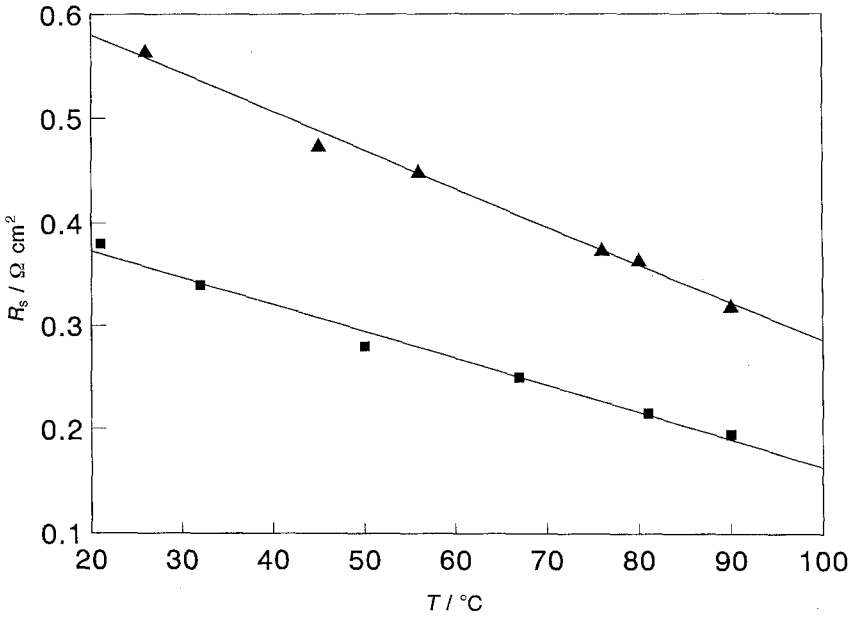

Fig. 5. Comparison of the series resistance values for the A and B assemblies at various temperatures. Key: (■) paste process; (▲) conventional.

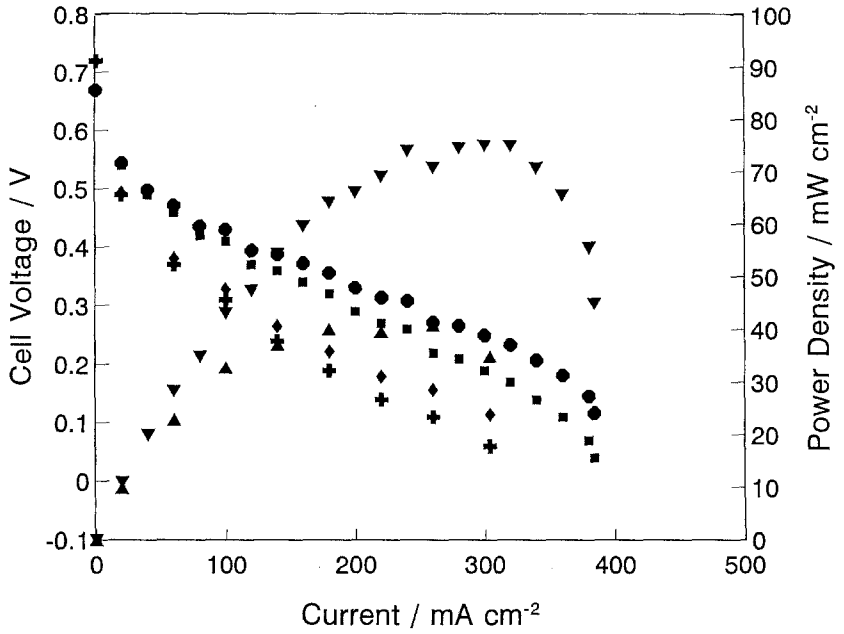

Fig. 6. DMFC polarization curves for the M&E assemblies prepared according to method A (✙) and method B (◆) together with their respective *iR*-free curves (■, method A; ●, method B) and electrical power densities (▲, method A; ▼, method B).

observed that the cell performance increased during the first day of operation and reached a steady state level during the second day. The uncompensated resistance (R_u) was measured by the current interruption method at high current densities. The R_u values were close to the series resistance determined by a.c.-impedance at the same temperature. A comparison of the steady-state current–potential behaviour for the M&E assemblies prepared according to the different procedures is shown in Fig. 6. The *iR*-free polarization curves are also reported together with the electrical power densities. It can be observed that the M&E assembly prepared according to the 'paste process' (B), i.e. with the ionomer acting both as binder and as ionic electrolyte in the catalyst layer, shows an increased electrochemical activity in the overall range of current densities. This increase in performance is only in small part due to the decrease in the uncompensated resistance. In fact, the power densities obtained from *iR*-free polarization curves for the B assembly is about twice that of the A assembly. The most significant increase in activity for the B assembly occurs in the activation region (Fig. 6) and may be related to the larger extension of the three-phase reaction zone on both cathode and anode sides that favourably influences the performance at low current density [6]. Mass-transport limitations are observed in the galvanostatic polarization of the B assembly at high current densities (Fig. 6).

It was not possible to attribute unequivocally these transport limitations to the anodic process. In fact, an increase in the CH_3OH flux produced an increase in fuel cross-over through the membrane.

The 'paste process' preparation method is not yet optimized for the direct methanol fuel cell and further improvements can be achieved in the kinetic and mass-transport properties. On the other hand, only a small improvement may be obtained for the uncompensated resistance as operation is close to the limit imposed by the Nafion® 117 membrane. It might be thought that the use of thinner perfluorosulfonic membranes can reduce the ohmic drop, yet this would increase the methanol cross-over, with consequent cathode poisoning.

3.4. *Scanning electron microscopy analysis*

Scanning electron microscopy was carried out on a few portions of the 50 cm^2 active area M&E assemblies after the electrochemical testing. No significant differences in morphology and chemical composition were observed among the various portions of each M&E assembly. The M&E assembly prepared according to the conventional method (A) is shown in Fig. 7. Five characteristic regions can be observed in the micrograph. The cathode backing layer comprises

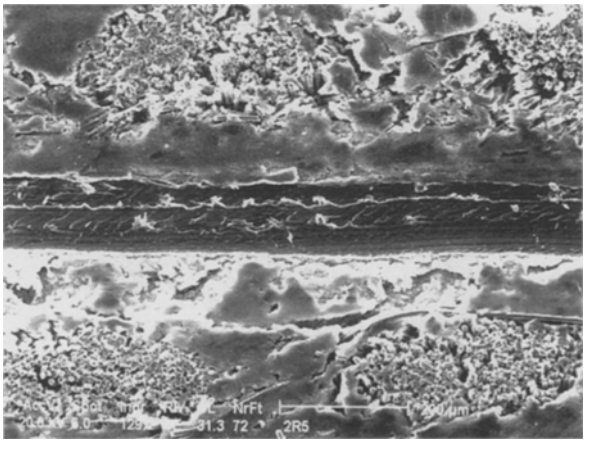

Fig. 7. SEM micrograph of a cross section of the M&E assembly prepared by method A; anode (top); cathode (bottom).

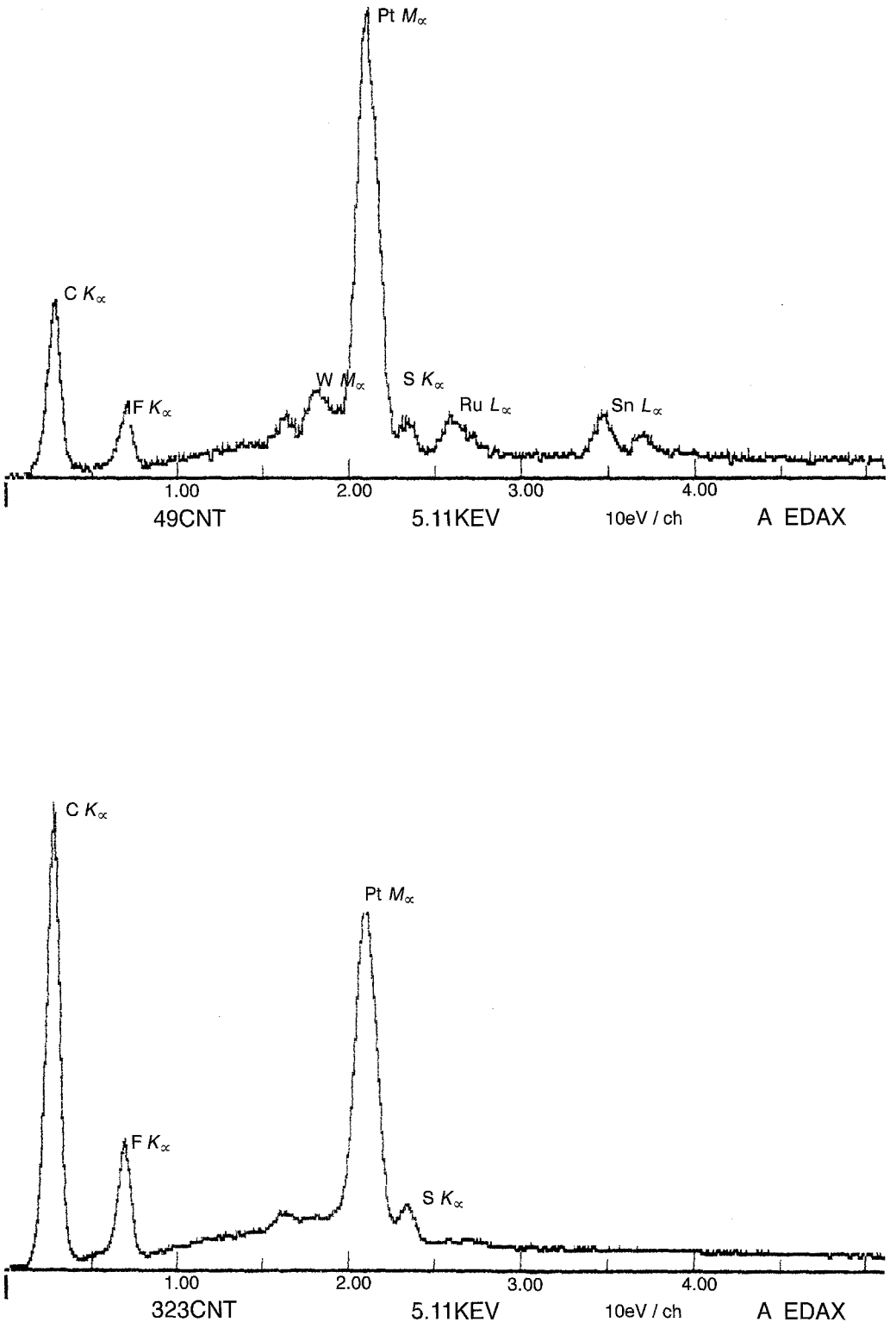

Fig. 8. Typical EDX spectra of the anode (a) and cathode (b) catalyst layers in Fig. 7.

carbon cloth fibre regions with stitch holes filled with the carbon black-based hydrophobic diffusion layer. The cathode catalyst layer, about 90 μm thick, is in close contact with the Nafion® membrane and with the diffusion layer. The observed thickness for the Nafion® membrane (about 120 μm) is smaller than the original thickness of the purchased membrane, probably due to the presence of an overlapping region with the catalyst and to the compacting load used during the M&E assembly formation. A morphology similar to the cathode side is observed at the anode for both catalyst and backing layer. The anode and cathode catalyst layers have the same thickness even though the Pt loading in the anode is about twice that of the cathode. Figure 8 shows two typical EDAX spectra of the anode and cathode catalyst layers, respectively, in the M&E assembly obtained by method A. The peaks related to C, F, W, Pt, S, Ru and Sn in the anode layer and C, F, Pt and S in the cathode layer respectively, are well defined. The chemical profile of a few significant elements along the M&E assembly cross section is reported in Fig. 9.

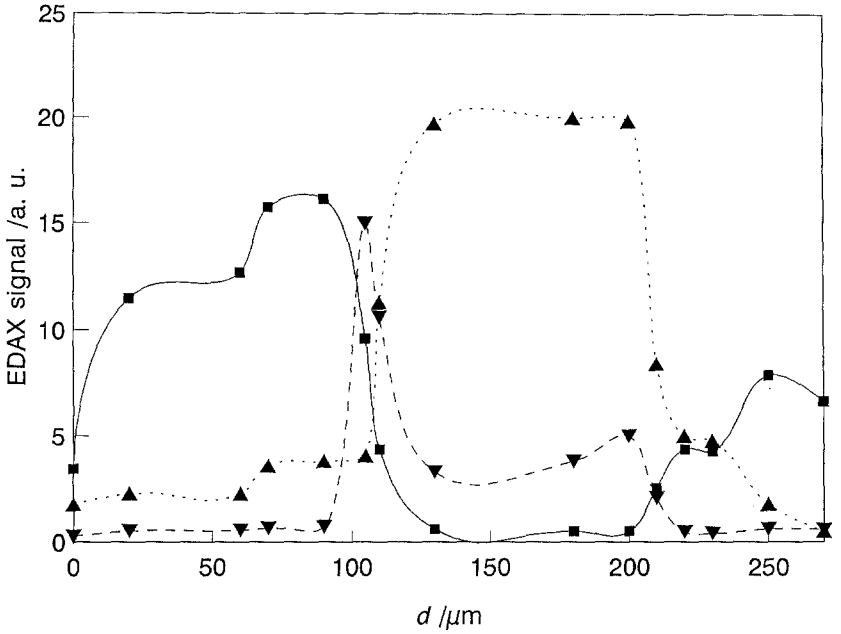

Fig. 9. Chemical profile along the cross-section of the M&E assembly prepared by method A. Key: (■) Pt; (▲) F; (▼) S.

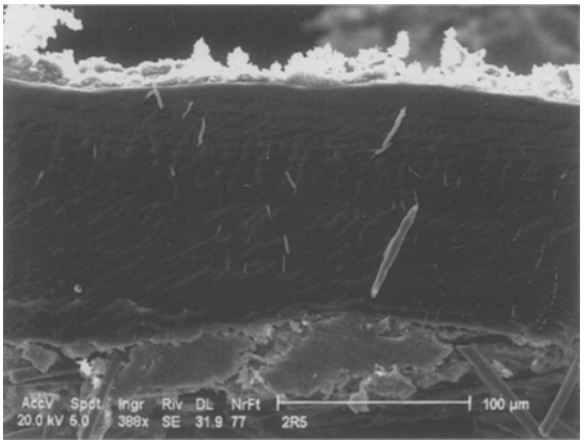

Fig. 10. SEM micrograph of a cross-section of the M&E assembly prepared by method B; anode (bottom); cathode (top).

It is observed that the sulfur signal, characteristic of the ionomer and membrane, decreases sharply, going from the membrane edge towards the interior of the anode and cathode catalyst layers. Hence, only a small part of the catalyst layer close to the membrane is in contact with the Nafion® ionomer.

A different morphology is observed for the M&E assembly prepared according to method B (Fig. 10). The catalytic layers appear significantly thinner and more irregular with respect to the former, whereas the Nafion® membrane appears to be thicker (average dimension, 150 μm) although the compacting load in the method B is significantly higher. The observed average dimension for the anode (bottom) and the cathode (top) layers is 50 and 25 μm, respectively (Fig. 10). Yet, the SEM observation at higher magnification showed that the catalyst layers are

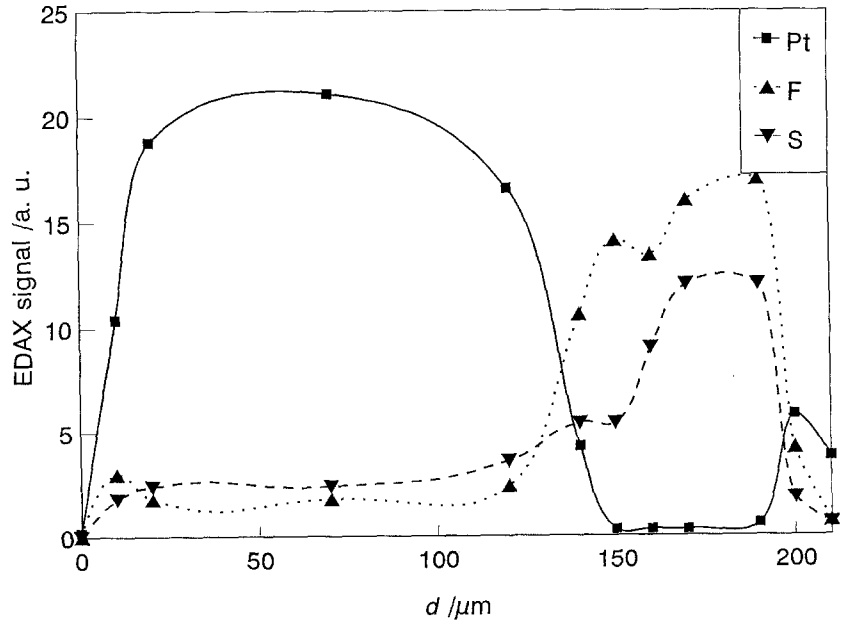

Fig. 11. Chemical profile along the cross-section of the M&E assembly prepared by method B.

interpenetrated with the membrane (not shown). This produces the previously observed effect, i.e. a decrease in thickness of the catalytic layers and a thicker membrane. A precise identification of the membrane–catalytic layer boundaries is not possible; EDAX analysis further supports this evidence. The chemical profile of the M&E assembly prepared according to method B is shown in Fig. 11. The sulfur signal related to the presence of the Nafion® ionomer is almost constant throughout the catalytic layers.

4. Conclusions

A significant improvement in the electrochemical performance of DMFCs is obtained by employing the 'paste process' for the M&E assembly fabrication. The improvement affects both the activation and ohmic controlled regions of the polarization curves. According to SEM analysis, this effect is probably due to the extension of the three-phase reaction zone and to an improved bonding between membrane and catalytic layer. The 'paste process' plays a favourable role in DMFCs as it produces a specific improvement in the activation-controlled region where the poor activity of the methanol oxidation catalyst affects the performance significantly.

The role of Pt promoters towards methanol oxidation has been widely investigated in the literature [11–17]. Our TEM analysis of the Pt–Ru–Sn–W/C catalyst suggests that, beside Pt-alloys, a catalytic role may be played by the overlapping of Pt f.c.c. lattice with nanocrystalline SnO_2 [7, 18], amorphous RuO_2 [7, 17] and/or WO_2/WO_3 [7, 19] particles. This mechanism is further supported by previous investigations of the Pt–SnO_2 [18], Pt–RuO_2 [17] and Pt–WO_3 [19, 20] bimetallic systems for methanol oxidation.

References

[1] S. Surampudi, S. R. Narayanan, E. Vamos, H. Frank and G. Halpert, A. LaConti, J. Kosek, G. K. Surya Prakash and G. A. Olah, *J. Power Sources* **47** (1994) 377.

[2] Siemens GmbH, Erlangen, Germany, European Community Report, Project JOU2- CT92-0104, Brussels, Feb. (1995).

[3] A. K. Shukla, P. A. Christensen, A. Hamnett, M. P. Hogarth, *J. Power Sources* **55** (1995) 87.

[4] M. S. Wilson and S. Gottesfeld, *J. Appl. Electrochem.* **22** (1992) 1.

[5] M. S. Wilson, J. A. Valerio and S. Gottesfeld, *Electrochim. Acta* **40** (1995) 3551.

[6] M. Uchida, Y. Aoyama, N. Eda and A. Ohta, *J. Electrochem. Soc* **142** (1995) 463.

[7] A. S. Aricò, Z. Poltarzewski, H. Kim, A. Morana, N. Giordano and V. Antonucci, *J. Power Sources* **55** (1995) 159.

[8] E. A. Ticianelli, C. R. Derouin, A. Redondo and S. Srinivasan, *J. Electrochem. Soc.* **135** (1988) 2209.

[9] V. Radmilovic, H. A. Gasteiger and P. N. Ross, Jr., *J. Catal.* **154** (1995) 98.

[10] B. E. Warren, 'X-ray Diffraction', Addison-Wesley, Reading, MA, (1969).

[11] H. A. Gasteiger N. Markovic, P. N. Ross, Jr. and E. J. Cairns, *J. Phys. Chem.* **97** (1993) 12020.

[12] B. Beden, F. Kadirgan, C. Lamy and J. M. Leger, *J. Electroanal. Chem.* **127** (1981) 75.

[13] A. Aramata, I. Toyoshima and M. Enyo, *Electrochim. Acta* **37** (1992) 1317.

[14] S. Wasmus and W. Vielstich, *J. Appl. Electrochem.* **23** (1993) 120.

[15] M. M. P. Janssen and J. Moolhuysen, *Electrochim. Acta* **21** (1976) 869.

[16] S. A. Campbell and R. Parsons, *J. Chem. Soc., Faraday Trans.* **88** (1992) 833.

[17] A. N. Buckley and B. J. Kennedy, *J. Electroanal. Chem.* **302** (1991) 261.

[18] A. S. Aricò, V. Antonucci, N. Giordano, A. K. Shukla, M. K. Ravikumar, A. Roy, S. R. Barman and D. D. Sarma, *J. Power. Sources* **50** (1994) 295.

[19] A. K. Shukla, M. K. Ravikumar, A. S. Aricò, V. Antonucci, N. Giordano and A. Hamnett, *J. Appl. Electrochem.* **25** (1995) 528.

[20] Shen and A. C. C. Tseung, Proceedings of the 186th meeting of the Electrochemical Society, vol. 93-1, Spring meeting, Extended abstract 576, Honululu, Hawaii, 16–21 May (1993).